XLIII CILAMCE
21–25, November, 2022
FOZ DO IGUAÇU – PR – BRAZIL

Core flood in porous micromodel made of glass

Jordana Colman[1], Fernanda Oliveira Hoerlle[1], Agatha Densi dos Santos Francisco[2], Raquel Machado Fedrizzi[3], José Luís Drummond Alves[1], Paulo Couto[1]

[1]*Dept. Civil Engineering, Federal University of Rio de Janeiro*
149, Athos da Silveira Ramos Avenue, Technology Center – room B- 101 – Fundão Island, mailbox 68506, CEP: 21941-909, Rio de Janeiro – RJ
jordana.colman@petroleo.ufrj.br, fernandahoerlle@petroleo.ufrj.br, jalves@lamce.ufrj.br, pcouto@petroleo.ufrj.br
[2]*Dept. of Chemistry, Federal University of Rio de Janeiro*
149, Athos da Silveira Ramos Avenue, Technology Center – room B- 101 – Fundão Island, mailbox 68506, CEP: 21941-909, Rio de Janeiro – RJ
agathadensi@petroleo.ufrj.br
[3]*Dept. Nanotechnology Engineering, Federal University of Rio de Janeiro*
2030, Horácio Macedo Avenue, Technology Center Building, room I-127, University City. CEP: 21.941-972 Rio de Janeiro - RJ.
raquelfedrizzi@petroleo.ufrj.br,

Abstract. Research using microdevices related to the flow in porous media are widely developed by the oil industry, aiming to understand the behavior of fluids, the interactions between the phases and the porous structure, and to increase the hydrocarbon recovery factor from the reservoirs. The objective of this work was to reproduce core flood test that was done on a rock but using a microdevice and the same fluid from the Brazilian pre-salt. Complex porous mesh micromodel was obtained through simulation, made of glass, and aged with crude oil, thus changing its wettability for oil wetting. Synthetic desulfated seawater (DSW) was injected as secondary recovery, at room temperature, with a flow rate of 1cm3/h and a bump flow of 2cm3/h. The experiment was recorded with high resolution images and a computer simulation was performed for the DSW velocities inside the micromodel. As a result of the image analysis, the recovery factor was calculated, which after the injection of 100 pore volumes was approximately 11,21 %. With the increase in flow, 7,92 % more oil was produced. With this, the fabricated microdevice has shown that it can be used to better understand fluid distribution and oil production in a core flood test.

Keywords: core flood, micromodel, porous media, oil, DSW.

1 Introduction

Oil production every decade needs to be increased due to the requirement to use this material in the most diverse branches of industry and mainly in the form of energy. Advanced oil recovery has been increasingly studied so that the demand for this material is met and its scarcity does not happen, according to BP [1]. To increase the recovery factor of oil wells, the field of microfluidics and porous micromodels have been increasingly used in studies in oil and gas, according to CRUZ [2] and ANBARI [3].

These microdevices can be applied in Enhanced Oil Recovery (EOR) studies, as they allow the observation of interactions between rock-fluid and fluid-fluid at the pore scale, also according to CRUZ [2]. Core flood experiments are expensive, use a large amount of material, take time to present results, this same experiment can be performed on a microscale faster, using less material resources and, if the micromodel was manufactured in transparent material, it allows the visualization of the flow, thus enabling the study of fluid-fluid and rock-fluid interaction (MEIJA [4]).

Another utility of the microchannel is that, due to the laminar flow, the transport of liquids is predictable and

can be easily observed thanks to the transparent nature of the microchips. The microfluidic ecosystem needs to have some basic parts which include inlet for fluids, a pump system to move these fluids through the microchips along with sensors to determine pressure and flow rates at the inlet and outlet of the microchips. The whole environment has to be executed very delicately and in a controlled way, as mentioned by GOGOI [5].

Typically, the first step in a core flood is to perform characterization experiments to obtain the permeability and porosity of the sample. Permeability is calculated using Darcy's law using measured pressure drops (the difference between the inlet and outlet pressures) at steady state, the core dimensions, and the fluid viscosity as inputs (MEIJA [4]).

To meet the objective of this study, which aims to perform a core flood test on a porous micromodel made of glass, the microdevice produced for this work was based on sandstone data using the degree of sediment selection and standard deviation, according to the FOLK literature [6] (1966) and generated through computer simulation. Its glass fabrication was carried out through chemical corrosion and sealed with an optical glue known as Norland Optical Adhesive (NOA81).

Several processes were carried out to achieve the calculation of the recovery factor of the micromodel studied. Velocity simulation, wettability study and image treatment were fundamental steps for the satisfactory result presented.

2 Materials and methods

2.1 Porous mesh simulation

To obtain a complex mesh, which will be used to manufacture or microdevice, several techniques can be applied within the parameters of representativeness of the real rock, such as micrography of thin sections described by ZUO [7] and KHORIDIAN [8] and X-ray microtomography (micro-CT), according to ANBARI [3]. But computer programs also help a lot in this construction.

These programs are based on mathematical geometries such as Triang Delaunay, as cited by GUNDA [9] Voronoi Diagram cited by KOU [10] and WU [11]. This work used a granulometric distribution and degree of selection to generate the porous media, following data from the sandstone literature of FOLK [12,13,14]. A program implemented in MATLAB software was written and required by researcher Enno de Vries, a doctoral student at the University of Utrecht in the Department of Earth Sciences. Input data provided according to sandstone literature, with that a network of deformed grains as well as input data, generated a CAD file. This file was opened in AutoCad to finalize the details of the input and output microchannels in the micromodel. The Fig. 1 shown shows a schematic of the finalized steps1 and a micromodel, with a porous mesh 10 mm by 10 mm. After the design is ready, the fabrication proceeds in different stages of the material used to make micromodels. This same porous mesh was used among other studies, as can be seen in CRUZ [3] and SARAIVA [15].

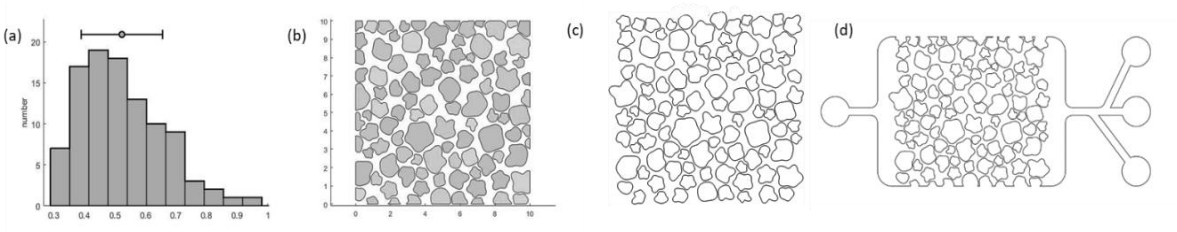

Figure 1. (a) Particle size distribution generated by the computational method. (b) Pore network generated from the input data. (c) The CAD file created from the simulation results (d) design of the porous mesh micromodel after completion in AutoCad.

2.2 Simulation of the velocity of the fluid injected into the porous micromodel

After obtaining the porous mesh by simulation with MATLAB, adding the wells and the input and output microchannels in AutoCad, the structure for fabrication and computer simulation is finalized, as shown in Fig. 1d.

This finished file was used to simulate fluid flow within the porous micromodel. The computational tool used was COMSOL. As it is a bench-top experiment, at room temperature, after mesh refinement, the input velocity value was added based on literature data. such as the study by RIAZI [16].

2.3 Manufacture of the porous glass microdevice

For the bench-top experiment in question, a glass micromodel was fabricated by chemical corrosion. Making glass micromodels is a delicate and highly complex process. Each manufacturing method using glass requires different substrates and different techniques because it is a fragile material at the pore scale.

In this manufacturing process, we count on the collaboration of the National Nanotechnology Laboratory (LNNANO), which is part of the National Center for Research in Energy and Materials (CNPEM), in Campinas.

Several processes were followed until the completion of the microdevice. They were deposited on the glass slide, thin film of chromium, photoresist, transferred through a photoaligner to the porous structure, baths with acids and washing with removers of the deposited materials.

The chemical attack takes place inside a fume hood with a bath of hydrofluoric acid (HF), ammonium fluoride (NH4F) and hydrochloric acid (HCl) in a ratio of 1:41:1 (v/v/v). In the buffer, the glass slide was immersed, followed by another bath with HF, both under agitation and, later, other baths to remove the remaining photoresist, chromium, and other residues.

An important step in completing the microdevice is sealing. For the porous micromodel, this step used an optical glue called NOA81 (Norland Optical Adhesive 81). This glue is easy to cure, transparent and resistant to organic solvents. In this case, the porous structure is at the base of the glass, and NOA81 serves only as an adhesive material, between the base and the lid (also made of glass). The porous micromodel can be seen in Fig. 3.

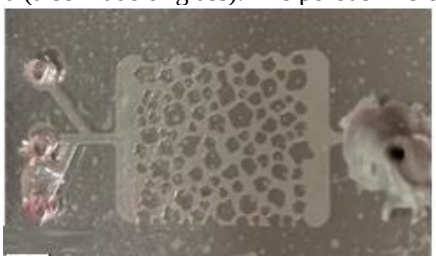

Figure 3. Micromodel made of glass and sealed with NOA81.

At the time of sealing, the optical adhesive NOA81 was used between the glass plates. To verify how much this material could influence the moment of synthetic desulfated seawater (DSW) injection after the aging process, a study on the wettability of NOA81 was carried out.

2.4 Aging process of the microdevice

An important step in oil recovery experiments is aging the pore system with crude oil. In micromodels this is a challenging process because the oil eventually evaporates from the grid openings, which would add an undesirable phase, air; as described in SAADAT [17]. To solve this problem, a new configuration was developed, in which a plastic tube was installed at the inlet and outlet of the microdevice. Then the syringe pump was connected to the system and oil was injected. After the micromodel was fully saturated with oil, the system was placed inside an oven at 60°C for 30 days to invert the wettability of the glass to a wetter state with oil, as performed by DREXLER [18]. The syringe pump was then disconnected, and the plastic tube was twisted to prevent oil loss.

2.5 Evaluation of wettability in the microdevices

The wettability in the microdevices fabricated from glass and NOA81 was evaluated through contact angle tests performed in the DSA 100E equipment (Kruss) at 25 °C and atmospheric pressure. The aging process in the NOA81 slab using crude oil occurred in static mode in the oven for 30 days at 60 °C. Afterward, the excess oil in the NOA81 slab was removed with heptane and dried in the oven. Then, it measured the contact angle between NOA81 – fluids interfaces.

3 Results

3.1 Porous Mesh

After placing the input data in MATLAB, according to HU [19] for sandstone rock, the simulation result

being passed through AutoCad to adjust the input and output channels, the porous micromodel with this process completed can be seen in Fig. 5.

In this mesh we have the smallest grain with a radius of 5 µm, a minimum distance between grains of 65 µm, final porosity of 0.403, porous volume of 1.2 µl with a porous mesh in the size of 10 mm by 10 mm.

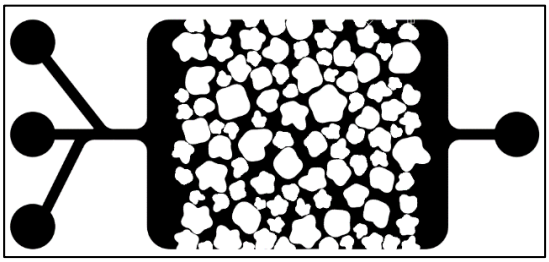

Figure 5. Porous mesh obtained from sandstone input data in MATLAB.

3.2 Simulation of the fluid velocity inside the Micromodel

As a way of verifying the interaction of the fluid with the microdevice, the velocity of the fluid injected inside it was simulated. As we can see in Fig. 6, velocities are higher at pore throats and lower at other points. Thus showing, according to Darcy's Law, that the permeability of the micromodel is low.

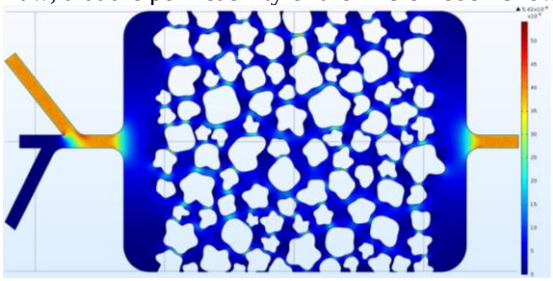

Figure 6. Simulation in COMSOL of the velocity of the fluid injected into the porous micromodel

3.3 Evaluation of wettability in the microdevices

Figure 7 shows the preliminary results of contact angle tests. It is possible to observe that the aging process became the NOA81 slab more oil-wet than the un-modified. In other words, the water drops had significant repulsion to aged NOA81 surfaces, whereas the oil drops exhibited a high affinity for them. Some authors consider oil-wet surfaces with contact angles above 90 °C and water-wet ones with contact angles below 90 °C when the standard fluid is water, and the opposite is true (Sheng [20]; Tiab and Donaldson [21]). Therefore, the aging process altered the wettability of the NOA81 slab to oil-wet. It is an adequate scenario to study the EOR process.

Figure 8 shows the contact angle in the NOA81 aged slab in the presence of water and DSW solution. These scenarios evaluated the wettability of NOA81 surfaces in the same conditions as the microdevice system. As observed in the preliminary results, NOA81 aged surfaces have also exhibited oil-wet behavior. However, in the presence of secondary injection water (DSW), there was an alteration in the wettability NOA81 slab. The divalent ions such as Mg^{2+} and Ca^{2+} present in the DSW solution are appointed in the literature as responsible for interacting with oil compounds and changing the wettability' of rocks through the ion-pair mechanism (LASHKARBOLOOKI [22,23,24]). Based on these results, it is possible to observe the same tendency.

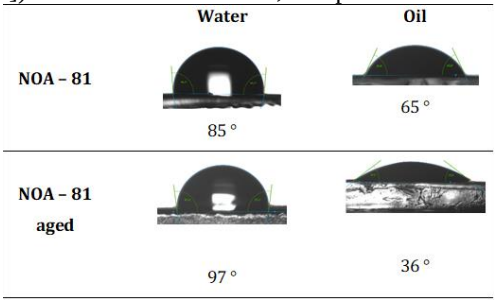

Figure 7. Contact angle between oil or water drops and NOA81 slab pure or aged.

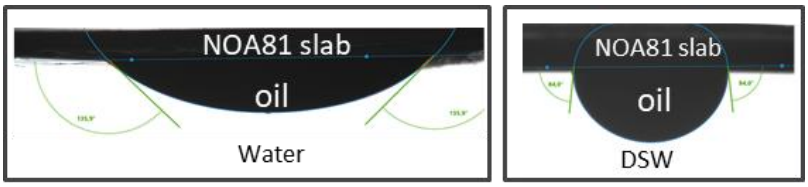

Figure 8. Contact angle between NOA81 slab - oil drop immersed in water or DSW solution.

3.4 Core flood in aging micromodel

As the aging process ended (Fig. 9), the micromodel saturated with crude oil was removed from the oven and taken to the experimental bench, which is composed of: of pump and syringe, camera to capture high resolution images, computer, and support base for the microdevice. In Fig. 9 the arrows point in the fluid flow direction, DSW.

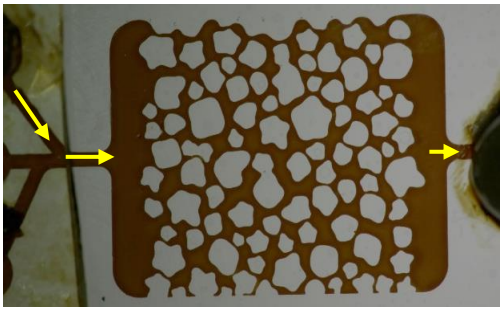

Figure 9. Aging process finalized and already positioned on the experimental stand; the arrows point towards the injection of the DSW.

With the connection already installed and connected to the syringe pump, the DSW injection was started with an initial flow of 1 cm^3/h. After injecting 100 porous volumes (PV), the injection flow rate was bump flow to 2 cm^3/h, and the same volume of fluid was injected. Fig. 10a shows the beginning of DSW injection, Fig. 10b shows the micromodel after 100 PV is injected, Fig. 10c the beginning of DSW injection with a bump flow of 2 cm^3/h and Fig. 10d shows the end of the experiment. Analyzing the set of photos in Fig. 10, we can observe that the fluid reaches a preferential path, on the right side of the microdevice, and in this path, the velocity is increased, presenting a lower fluid-oil interaction. With the increase in flow, the DSW begins to reach other points within the micromodel that was previously more concentrated in one region. But even the DSW reaching other points, in the preferential path still presents the presence of oil that could be displaced.

During the entire experiment, photos were taken with a high resolution camera to later, with the help of the ImageJ computer program, treat the images and calculate the oil recovery factor. Photos as in Fig. 10, show the oil displacement within the micromodel. Through the treatment of these images, this displacement can be measured and quantified. Based on the filled spaces, the program highlights where the oil is and, through a command, the quantification of fluid that was displaced appears in percentage of area. Fig. 11 shows a finalization of the DSW injection process and the image processing carried out through ImageJ. In Fig. 11a is the 8-bit image in Fig. 11b is the oil being detached to calculate the area being occupied by it, and in Fig. 11c is the processing measuring the area with oil and the calculated recovery factor of each fluid injection step is shown in Tab. 1.

As seen in Tab. 1, the area occupied by the oil decreased as the DSW injection took place, from the beginning of the injection after 100 PV the percentage of oil area decreased, thus resulting in a recovery factor of 11.29%. After the bump flow, the area occupied by the oil decreased, resulting in a recovery factor of 7.21%. This demonstrates that this core flood test can identify the existence of trapped oil due to the capillary effect.

Table 1. Recovery factor calculated at the end of each DSW injection step

	Total area	Oil area	Recovery Factor
Start	130,62	70,02 (53,61%)	
100 PV	130,61	55,76 (42,23%)	11,29%
Finished	130,61	45,07 (34,31%)	7,92%
			19,21%

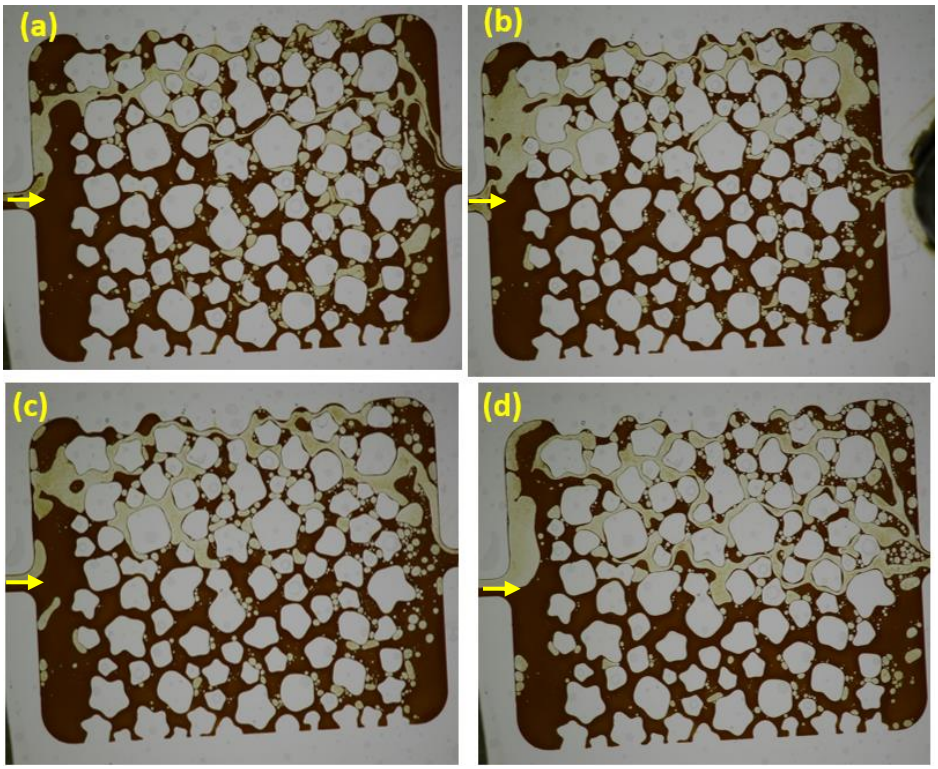

Figure 10: (a) start of DSW injection with a flow rate of 1 cm^3/h, (b) 100 PV of DSW injected at 1 cm^3/h, (c) start of flow increase to 2 cm^3/h and (d) completion of the DSW injection.

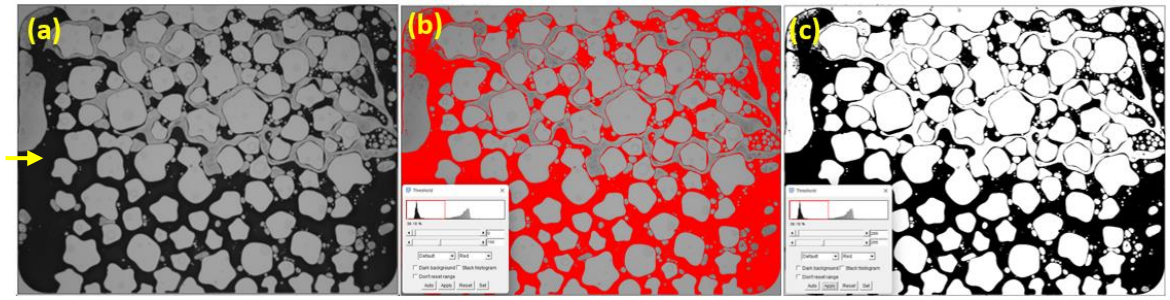

Figure 11. Image processing of DSW injection completion using ImageJ.

4 Conclusions

The fabricated micromodel proved to be satisfactory for bench core flood testing. With the possibility of visualizing the experiment, we can see that the DSW reached a preferential path and after a bump flow, it spread reaching other grains and increasing the recovery factor. It was also possible to observe the capillary effect inside the device.

The oil recovery factor in the injection experiments corroborated the wettability measurements obtained in the NOA81 contact angle tests. This polymer proved to be both efficient for bench testing and for sealing the microdevice.

For the study of velocity simulation, we can observe points where the velocity is higher and a good permeability of the micromodel generated with the input data of a sandstone.

The improvement of this experiment may result in future work with good results and comparing and assisting in core flood tests in high pressure and temperature ovens.

Acknowledgements. This research was carried out in association with the ongoing R&D project registered as ANP nº 20163-2, “Análise Experimental da Recuperação de Petróleo para os Carbonatos do Pré-sal do Brasil

através de Injeção Alternada de CO2 e Água" (UFRJ/Shell Brasil/ANP), sponsored by Shell Brasil under the ANP R&D levy as “Compromisso de Investimentos com Pesquisa e Desenvolvimento”.

Authorship statement. I declare, as the author of the manuscript, that I participated in the construction and formation of this work, and I assume public and ethical responsibility for its content.

References

[1] BP. BP Statistical Review of World Energy 2016. London: BP Statistical Review of World Energy, 2016. Disponível em <http://www.bp.com/statisticalreview>. Acesso em 20 de agosto de 2021
[2] CRUZ, F.A. Flow visualization of silica nanofluid injection for Enhanced Oil Recovery in a micromodel based on well-sorted grain-size porous media. Dissertação (Mestrado em Engenharia da Nanotecnologia) - COPPE/UFRJ. 2019.
[3] ANBARI, A., CHIEN, H.-T., & et all. (n.d.). Microfluidic Model Porous Media: Fabrication and Applications. Vol. 14, No. 18, p. 1703575, 2018.
[4] MEIJA, Lucas, Zu, Peixi & et all. Coreflood on a chip: Core-scale micromodels for subsurface applications. Vol. 281, No. 13, p. 118716, 2020. https://doi.org/10.1016/j.fuel.2020.118716
[5] GOGOI, S., GOGOI, SB Revisão sobre estudos microfluídicos para aplicação EOR. J Petrol Explor Prod Technol 9, 2263-2277 (2019). https://doi.org/10.1007/s13202-019-0610-4.
[6] Folk, R. L. A review of grain-size parameters. Sedimentology, 6 (1966), pp. 73-94. https://doi.org/10.1111/j.1365-3091.1966.tb01572.x
[7] ZUO, Lin, Changyong Zhang, Ronald W. Falta, Sally M. Benson. Micromodel investigations of CO2 exsolution from carbonated water in sedimentary rocks, Advances in Water Resources, Volume 53, 2013, Pages 188-197, ISSN 0309-1708, https://doi.org/10.1016/j.advwatres.2012.11.004.
[8] H. Khorshidian, Lesley A. James, Stephen D. Butt. Demonstrating the effect of hydraulic continuity of the wetting phase on the performance of pore network micromodels during gas assisted gravity drainage, Journal of Petroleum Science and Engineering, Volume 165, 2018, Pages 375-387, ISSN 0920-4105, https://doi.org/10.1016/j.petrol.2017.11.016.
[9] N. S. GUNDA, et al. Reservoir-on-a-Chip (ROC): A new paradigm in reservoir engineering. Lab on a chip, v. 11, p. 3785–3792, 21 Nov. 2011.
[10] KOU, X. Y. and Tan, S. T. A Simple and Effective Geometric Representation for Irregular Porous Structure Modeling, October 2010, Butterworth-Heinemann, USA. Vol. 42, No. 10, https://doi.org/10.1016/j.cad.2010.06.006.
[11]M, WU, Xiao, F., Johnson-Paben, R. M., Retterer, S. T., Yin, X., & Neeves, K. B. (2012). Single-and two-phase flow in microfluidic porous media analogs based on Voronoi tessellation. *Lab on a Chip*, *12*(2), 253-261.
[12] FOLK, R.L. (n.d.). *Petrology of sedimentary rocks*. 1980.
[13] FOLK, R.L.; WARD, C. W. Brazos River bar, & WARD, C. W. Brazos River bar. (n.d.). A study in the significance of grain size parameters. *J. Sediment*.
[14] FOLK, R. L. (n.d.). A review of grain-size parameters. *Sedimentology*.
[15] T. C. SARAIVA. Análise da injeção de água de baixa salinidade na recuperação de óleo em microdispositivos de sistemas porosos de PDMS. Dissertação de Mestrado. Rio de Janeiro: UFRJ/COPPE, 2019.
[16] M. RIAZI, Mehran Sohrabi, Christian Bernstone, Mahmoud Jamiolahmady, Shaun Ireland, Visualisation of mechanisms involved in Co2 injection and storage in hydrocarbon reservoirsand water-bearing aquifers, Chemical Engineering Research and Design, Vol. 89, Issue 9, 2011, p. 1827-1840, ISSN 0263-8762, https://doi.org/10.1016/j.cherd.2011.03.009.
[17] M. SAADAT, et al. Development of a microfluidic method to study enhanced oil recovery by low salinity water flooding. ACS omega, v. 5, n. 28, p. 17521-17530, 2020.
[18] S. G. DREXLER. Study of the fluid-fluid and rock-fluid interactions: impact of dissolved co2 on interfacial tension and wettability for the brazilian pre-salt scenario. Tese de Doutorado Rio de Janeiro: UFRJ/COPPE, 2018.
[19] X. HU, et al. (Ed.). Physics of petroleum reservoirs. Springer Berlin Heidelberg, 2017.
[20] J. SHENG. 2010. Modern Chemical Enhanced Oil Recovery: Theory and Practice, Modern Chemical Enhanced Oil Recovery: Theory and Practice.
[21] D. TIAB, Donaldson, E.C., 2015. Petrophysics: Theory and Practice of Measuring Reservoir Rock and Fluid Transport Properties: Fourth Edition, Petrophysics: Theory and Practice of Measuring Reservoir Rock and Fluid Transport Properties: Fourth Edition. https://doi.org/10.1016/C2014-0-03707-0
[22] M. LASHKARBOLOOKI, Ayatollahi, S., Riazi, M., 2017. Mechanistical study of effect of ions in smart water injection into carbonate oil reservoir. Process Saf. Environ. Prot. 105, 361–372. https://doi.org/10.1016/j.psep.2016.11.022
[23] M. LASHKARBOLOOKI, Ayatollahi, S., Riazi, M., 2014. The impacts of aqueous ions on interfacial tension and wettability of an asphaltenic-acidic crude oil reservoir during smart water injection. J. Chem. Eng. Data 59, 3624–3634. https://doi.org/10.1021/je500730e
[24] M. LASHKARBOLOOKI, Riazi, M., Hajibagheri, F., Ayatollahi, S., 2016. Low salinity injection into asphaltenic-carbonate oil reservoir, mechanistical study. J. Mol. Liq. 216, 377–386. https://doi.org/10.1016/j.molliq.2016.01.051